Received: 1 July 2023 | Accepted: 22 August 2023

DOI: 10.1002/pamm.202300199

RESEARCH ARTICLE

Numerical optimisation of damage in extrusion processes

Fabian Guhr[1] | **Robin Gitschel**[2] | **Franz-Joseph Barthold**[1] | **A. Erman Tekkaya**[2]

[1]Institute of Structural Mechanics and Dynamics, TU Dortmund University, Dortmund, Germany

[2]Institute of Metal Forming and Lightweight Components, TU Dortmund University, Dortmund, Germany

Correspondence
Fabian Guhr, Institute of Structural Mechanics and Dynamics, TU Dortmund University, August-Schmidt-Str. 8, D-44227 Dortmund, Germany.
Email: fabian.guhr@tu-dortmund.de

Funding information
Deutsche Forschungsgemeinschaft, Grant/Award Number: 278868966

Abstract

Numerical optimisation is applied to rod extrusion in order to generate optimal parameter sets which result in reduced damage accumulation. A brief overview of academic applications for damage optimisation is given. Their restrictions are reflected upon, leading to the proposed framework utilising the commercial software Abaqus FEA, which enables optimisation of industrial problems with frictional contact. The framework is setup modularly to enable arbitrary choices of design variables, such as geometric parameters, and process parameters like friction coefficients or boundary conditions. The optimisation strategy is applied to forward hollow extrusion. Compared to forward rod extrusion, an additional design variable, that is, the mandrel radius, is introduced into the forming process, which increases the design space.

1 | INTRODUCTION

Complex components manufactured by cold forging enable economical and resource-efficient production with reproducible high quality. Forming, however, does not only define a components desired geometric shape, but also its properties to a large extent. For example, work hardening or the systematic introduction of compressive residual stresses are well-known in industry to produce components with increased performance. Besides these positive effect, ductile damage is induced into the components during forming. The term damage describes the nucleation, growth and coalescence of voids on the microscopical scale, compare [1]. Such voids are induced during forming, for example, at inclusions or through the fracture of hard phases, and continue to grow in size with increasing plastic strain. By specific modifications of existing forming processes, the accumulation of damage during forming can be reduced, which in turn increases the performance of the component, compare [2].

Improvements of already established forming processes can be achieved in a multitude of ways. By combining existing knowledge with experiments, certain process parameters can be altered and adapted to improve the considered process. With respect to damage reduction in forming processes for example, [3] laid out the necessary parameters for the process of forward rod extrusion that need to be changed in order to generate the same parts but with different damage characteristics. However, enhancements of this process were achieved manually, that is, by changing parameters in simulation and experiment by hand and analysing the results. Here, numerical based optimisation can be very beneficial because it automates these steps by finding optimal solutions. Additionally, a solution acquired this way may not be instinctively found by conventional means when, for example, the solution lies between typically investigated parameter sets.

While numerical optimisation of damage is applied to academic-type problems for structural optimisation in literature, compare [4–6], its application within industrial-like problems is only scarcely researched. In this work a framework

This is an open access article under the terms of the Creative Commons Attribution License, which permits use, distribution and reproduction in any medium, provided the original work is properly cited.
© 2023 The Authors. *Proceedings in Applied Mathematics & Mechanics* published by Wiley-VCH GmbH.

around the commercial software Abaqus FEA [7] is proposed, which handles the contact problems and runs the simulations, enabling numerical optimisation of forming processes.

2 | NUMERICAL DAMAGE OPTIMISATION

In this section, a brief overview of possible approaches within different settings of numerical damage optimisation is presented. Since the focus of this paper is on the application within industrial settings, that is, the cold forging process of rod extrusion, the first approach for academic-like problems is only briefly looked upon and the reader is forwarded to additional literature. The second approach describes the framework to optimise arbitrary problems for large-scale problems, utilised to generate the results in Section 3.

2.1 | Academic application

For the academic application of damage optimisation, sensitivity analysis is applied to a non-local damage model to derive the gradients and therefore enable gradient-based optimisation. Utilisation of a variational approach, compare [8], the total variation of the residual of the resulting two-field problem results in

$$\delta \boldsymbol{r} = \delta_{\boldsymbol{w}} \boldsymbol{r} + \delta_{\boldsymbol{s}} \boldsymbol{r} + \delta_{\boldsymbol{h}_n} \boldsymbol{r} = \boldsymbol{0}, \tag{1}$$

with mechanical and non-local damage residual $\boldsymbol{r}$, deformation $\boldsymbol{\varphi}$ and non-local damage $\boldsymbol{\phi}$ such that $\boldsymbol{w} = [\boldsymbol{\varphi}, \boldsymbol{\phi}]$, design $\boldsymbol{s}$ and state-dependent history-variables $\boldsymbol{h}_n$ at time step n. Consistent discretisation into a matrix form, denoted by bold faced upright Roman letters, and restructuring of the resulting equations allows the derivation of the sensitivity matrix $\mathbf{S}$, that is,

$$\delta \mathbf{w} = -\mathbf{K}^{-1}[\mathbf{P}\,\delta \mathbf{s} + \mathbf{H}\,\delta \mathbf{h}_n] = -\mathbf{K}^{-1}[\mathbf{P} + \mathbf{H}\mathbf{Z}_n]\delta \mathbf{s} =: \mathbf{S}\,\delta \mathbf{s}, \tag{2}$$

which describes how a system and its field variables $\mathbf{w}$ react due to a change in design $\mathbf{s}$. The matrices therein are the pseudo-load matrix $\mathbf{P}$ and the history sensitivity matrix $\mathbf{H}$. The additional matrix $\mathbf{Z}_n$ results from the total variation of the history field, that is,

$$\delta \mathbf{h} = \left[\frac{\partial \mathbf{h}}{\partial \mathbf{w}} \mathbf{S} + \frac{\partial \mathbf{h}}{\partial \mathbf{s}} + \frac{\partial \mathbf{h}}{\partial \mathbf{h}_n} \mathbf{Z}_n \right], \tag{3}$$

which requires iterative updates after each converged global Newton solution of time step $n + 1$, compare [9, 10]. Application of these gradients enables for minimisation and control of damage in analysed optimisation problems. A more detailed layout of this concept is presented in for example [4, 5]. However, this approach does not include the contact mechanics necessary for forming simulations. While research on sensitivity analysis with contact has been conducted in literature, compare [11, 12], its application to large-scale, non-linear materials is yet to be extended. This motivates the alternative approach chosen in the following section.

2.2 | Industrial application

In the industrial setting, for example, forming processes, the previously described approach is difficult to incorporate. Commercial software generally allows stable computation of complex processes, which may not necessarily be possible with academic software. Furthermore, if multiple processes are analysed and different material behaviour considered, the above approach requires renewed derivations of the gradients for the altered material behaviour. Hence, for the industrial application, a different approach is preferable.

The basis for this approach is the utilisation of commercial finite element (FE) software as the solver, that is, Abaqus FEA [7] in this case, and developing a framework to enable optimisation around this software. While it may be possible to utilise other commercial software to directly optimise such processes, the choice of Abaqus FEA as the solver boils

RIGHTSLINK

16177061, 2023, 3, Downloaded from https://onlinelibrary.wiley.com/doi/10.1002/pamm.202300199 by Technische Universitaet Dortmund Dezernat Finanzen und Beschaffung, Wiley Online Library on [24/10/2024]. See the Terms and Conditions (https://onlinelibrary.wiley.com/terms-and-conditions) on Wiley Online Library for rules of use; OA articles are governed by the applicable Creative Commons License

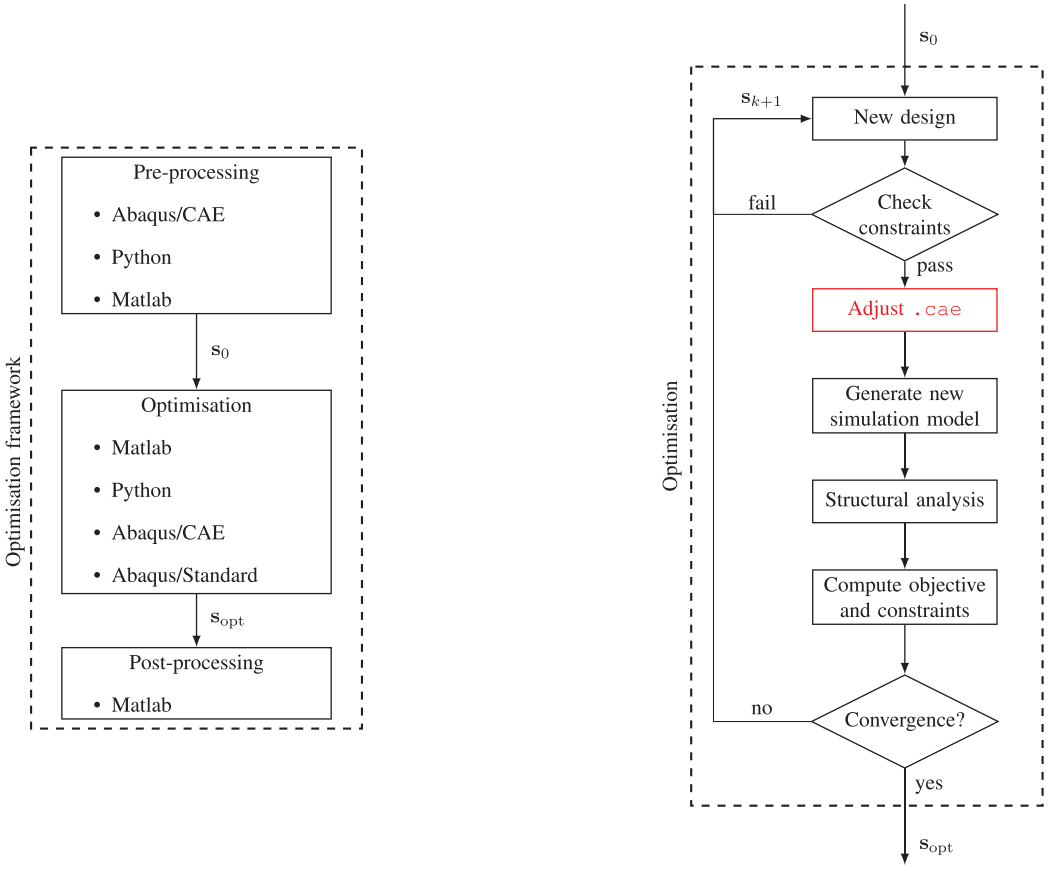

(A) Optimisation framework.

(B) Optimisation flow chart.

FIGURE 1 The optimisation framework and the flow chart of the optimisation routine. In red, the use of Abaqus/CAE to update the model.

down to ease the cooperation within the Collaborative Research Centre TRR188, the source of funding for this research. The overall setup is summarised in Figure 1A, while the detailed optimisation flow chart is presented in Figure 1B. The framework utilises three main components to enable optimisation:

1. Abaqus to run the simulations and to enable the definition of the design variables,
2. Python to extract the simulation data and to incorporate the updated design variables into the model after each iteration,
3. Matlab to handle the pre-processing, post-processing and simulation data, as well as to run the optimisation itself.

This approach is an extension to the implementation in [13, 14]. In this initial concept, applied to air bending, the input-file (`.inp`) of the simulation problem was directly modified to incorporate design changes. While this approach is easy to implement, it has its drawbacks regarding optimisation problems where for example, complex geometric definitions are changed. At that point, a mapping between the mesh used within the simulation and the one generated by the optimiser, outside the commercial simulation software, is required, which is not necessarily straight forward to deduct. In order to allow such optimisation problems to be handled easily, the changes are now directly applied to the model data base (`.cae`). This file includes all necessary data to model the simulation problem within the Abaqus/CAE GUI which at the end results in the creation of the input-file to run the simulation. The data stored in the data base can be accessed and changed by means of python scripting, which in turn directly results in automatically applied changes within Abaqus itself, circumventing necessary mappings for geometric modifications. To enable these, the design variables of the optimisation need to be parametrised within the `.cae`-model, which is prepared during pre-processing. Additionally, the areas within the model, where the objective function and possible constraints shall be evaluated, need to be defined. This is achieved by generating two sets within the Abaqus model. Finally, two kinds of python scripts need to be provided. The first script is used to make the changes in the `.cae`-model data base, wherein the newly generated design variables are used as

RIGHTSLINK

16177061, 2023, 3, Downloaded from https://onlinelibrary.wiley.com/doi/10.1002/pamm.202300199 by Technische Universitaet Dortmund Dezernat Finanzen und Beschaffung, Wiley Online Library on [24/10/2024]. See the Terms and Conditions (https://onlinelibrary.wiley.com/terms-and-conditions) on Wiley Online Library for rules of use; OA articles are governed by the applicable Creative Commons License

input variables. It is applied to the Abaqus model database within the optimisation and is called before each simulation during subsequent optimisation steps. The second script is required to evaluate the data stored in the output database. It evaluates the results, and outputs the data for the objective function and possible constraints. It is called after each finite element simulation.

The optimisation itself uses the optimisation toolbox within Matlab and can either employ several gradient-based strategies using *fmincon*, or the gradient-free method *fminsearch*, which utilises a Nelder-Mead simplex. For the problem types where this framework is applied, the latter showed better results, due to the previously described discontinuities introduced by the contact problems. However, this algorithm can generally not handle constraints. To treat these nonetheless, the penalty method is applied in two steps. The applied constraints can be generalised into two groups. The first type of constraints are simulation dependent, that is, the FE simulation has to be conducted until they can be evaluated, for example, stresses and strains. These constraints can be included by adapting the evaluated objective function, that is, increasing the objective function value J if a constraint c_i is not fulfilled, such that

$$J^{\text{pen}} = J + \sum_{i=1}^{n_c} \beta_c \, c_i, \tag{4}$$

with a problem dependent penalty parameter β_c and the number of constraints n_c. The second group of constraints are simulation independent and can be evaluated before running the FE simulation. These types of constraints can be for example, of geometric type and evaluated before running said simulation. Since the objective function is unknown at this point and therefore cannot be directly influenced, instead a high function value, that is, `Inf`, is returned. This forces the optimiser to treat the current iteration as unsuitable and to try a different step for the current iteration.

3 | RESULTS

In this section, the numerical setup and important parameters regarding the optimisation for hollow forward extrusion are described. Afterwards, the process is optimised to generate an optimal set of process parameters with the aim of a reduced damage accumulation during forming.

3.1 | Simulation and optimisation setup

For the exemplary optimisation, the process of forward hollow extrusion is chosen. Compared to the standard process of forward rod extrusion, a mandrel is inserted into the centre of the workpiece, with the aim of creating hollow extruded parts, see Figure 2. This figure shows the three main components of the process, that is, the die, the workpiece and the inner mandrel. The relevant process parameters regarding the optimisation are the final radius r_1, the mandrel radius r_m and the shoulder opening angle 2α. The additional process parameters, that is, the initial radius $r_0 = 15.1$ mm, the friction parameter $\mu = 0.04$ and the transition radius $r = 1$ mm, are kept constant throughout the optimisation. An additional characteristic parameter describing the process is the extrusion strain ε_{ex}, which gives information on the ratio of cross section

$$\varepsilon_{\text{ex}}(r_0, r_1, r_\text{m}) = \ln\left(\frac{d_0^2 - d_\text{m}^2}{d_1^2 - d_\text{m}^2}\right) = \ln\left(\frac{r_0^2 - r_\text{m}^2}{r_1^2 - r_\text{m}^2}\right). \tag{5}$$

The Abaqus/CAE model for this simulation is taken directly from the authors of [3] and adapted for the extended process. Furthermore, it is adapted for the optimisation framework, that is, the design variables are parametrised and the previously mentioned sets are defined. The workpiece is modelled with linear four-noded thermo-mechanically coupled axisymmetric elements CAX4RHT, while the die and the mandrel are modelled with CAX4RT elements. The elasto-plastic material behaviour and its flow curves at 20°C, 200°C and 400°C are obtained in upsetting tests of case hardening steel 16MnCrS5, to model the plastic behaviour within the simulation accurately. Contact between die and workpiece, as well as mandrel and workpiece, are of master-slave type, with Coulomb friction defined by the friction parameter μ between both parts, respectively.

RIGHTSLINK

16177061, 2023, 3, Downloaded from https://onlinelibrary.wiley.com/doi/10.1002/pamm.202300199 by Technische Universitaet Dortmund Dezernat Finanzen und Beschaffung, Wiley Online Library on [24/10/2024]. See the Terms and Conditions (https://onlinelibrary.wiley.com/terms-and-conditions) on Wiley Online Library for rules of use; OA articles are governed by the applicable Creative Commons License

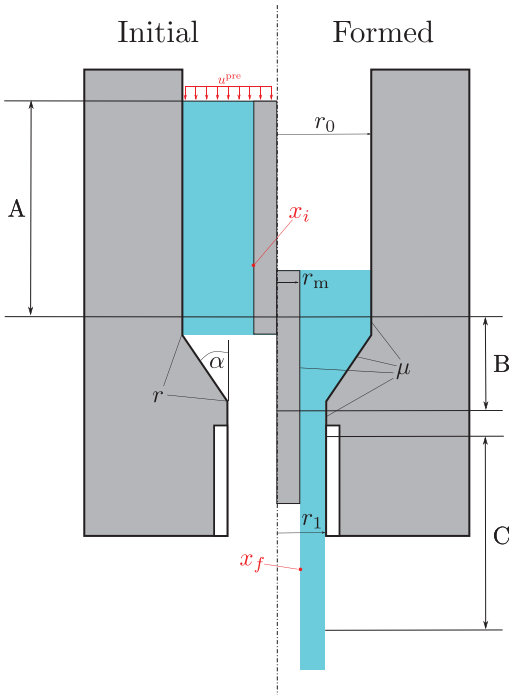

FIGURE 2 An illustration of the simulations conducted during the optimisation processes. The left part shows the initial configuration with the formed one on the right.

In Figure 2 two points are denoted in red. These indicate the approximate location of the chosen element for the evaluation of the objective function initially x_i and after forming x_f. This element has to fulfil certain conditions throughout the process. On one hand, it has to lie on the central axis of the workpiece, as this area is the most critical regarding damage accumulation. On the other hand, it is chosen such that it lies outside the forming zone at process initiation, transverses the forming area and finally is located within the steady-state region of the forming process after the simulation is finished. These three areas and their approximate location within the figure are denoted with the letters A, B and C, respectively.

The incorporated material model does not include damage behaviour. Therefore, the measurement from [3] is chosen as the objective of the optimisation model to minimise the resulting damage accumulation, that is,

$$\eta^{\text{mean}} = \frac{\int_{t_0}^{t_{\text{end}}} \eta(\bar{\varepsilon}^{\text{p}}(t))\, \dot{\bar{\varepsilon}}^{\text{p}}(t)\, \mathrm{d}t}{\int_{t_0}^{t_{\text{end}}} \dot{\bar{\varepsilon}}^{\text{p}}(t)\, \mathrm{d}t} \quad \text{with} \quad \eta = \frac{\sigma_{\text{h}}}{\sigma_{\text{vM}}}. \tag{6}$$

Therein, η denotes the well-known stress triaxiality, which is defined as the fraction between the hydrostatic stress σ_{h} and the von Mises equivalent stresses σ_{vM}. The measurement η^{mean} consequently captures the evolution of triaxiality during plastic forming, that is, the moment at which damage evolves throughout the forming process, compare [3].

3.2 | Optimisation with a variable mandrel radius

The chosen design variables for the optimisation problem encompass previously denoted process parameters $\mathbf{s} = [r_{\text{m}}, r_1, 2\alpha]$. The extrusion strain ε_{ex} of the process is introduced as a limiting side constraint. Since this constraint is of geometric type, it can be handled by validating its fulfilment before running the taxing FE simulation, as described in Section 2.2. The optimisation problem reads

$$\begin{aligned} &\underset{\mathbf{s}_l \le \mathbf{s} \le \mathbf{s}_u}{\text{minimise}} && \eta^{\text{mean}}(\mathbf{s}) \\ &\text{subject to} && 0.2 \le \varepsilon_{\text{ex}}(r_{\text{m}}, r_1) \le 1.4. \end{aligned} \tag{7}$$

RIGHTSLINK

16177061, 2023, 3, Downloaded from https://onlinelibrary.wiley.com/doi/10.1002/pamm.202300199 by Technische Universitaet Dortmund Dezernat Finanzen und Beschaffung, Wiley Online Library on [24/10/2024]. See the Terms and Conditions (https://onlinelibrary.wiley.com/terms-and-conditions) on Wiley Online Library for rules of use; OA articles are governed by the applicable Creative Commons License

TABLE 1 The table for the optimisation of forward hollow extrusion with a variable mandrel radius r_m.

s	dependent	fixed	s_l	s_u	initial (k=0)	intermediate (k=12)	optimum (k=75)
-	-	r_0/mm	15.1	15.1	15.1	15.1	15.1
r_1/mm	-	-	9.5	13.9	11.5	11.316	11.815
r_m/mm	-	-	6.7	11.6	9.5	9.703	10.517
-	ε_{ex}	-	0.2	1.4	1.188	1.373	1.399
$2\alpha/°$	-	-	30	150	60	58.839	30.012

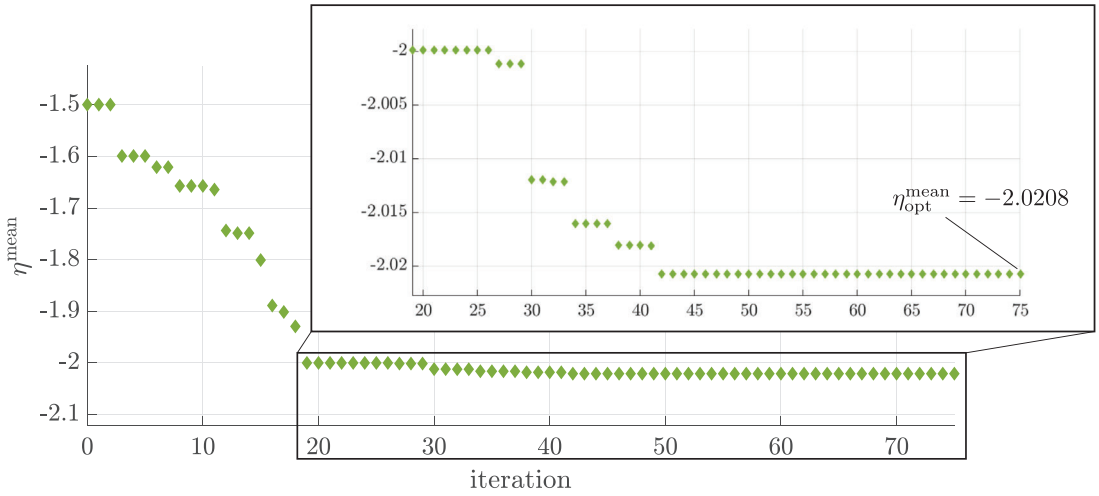

FIGURE 3 Objective function over iterations for the optimisation problem of forward hollow extrusion with a variable mandrel radius r_m. The framed area shows a zoomed-in depiction for the respective iterations with a rescaled ordinate.

The resulting, and some intermediate values, are listed in Table 1. The optimiser tries to maximise the extrusion strain initially, as this has the highest impact on the objective function, compare [3]. Since this value depends on two possible changes in the chosen design variables, intermediate results show that at first the final diameter r_1 is decreased, with the mandrel radius r_m also being increased to achieve a high extrusion strain. The shoulder angle remains mostly constant at the beginning and only decreases at later stages in the optimisation, indicating a lower impact on the objective value compared to the radii. After increasing the extrusion rate, the optimiser again increases the final radius r_1, while further increasing the mandrel radius r_m in order to remain at the bounded extrusion rate value of $\varepsilon_{ex,u} = 1.4$. This finally leads to the optimal design, see Table 1.

The iterative process in Figure 3 also shows the described behaviour. Throughout the optimisation, up to iteration 19, large jumps in the objective function can be seen, mostly due to the changes in radii. At this point, the design variables are close to the final optimal values and only small adjustments are made, leading to consequently small modification of the objective function, depicted in the zoomed-in part of Figure 3.

Interestingly, the final values of r_1 and r_m do not reach their respective bounds, indicating that it may be beneficial for this forming process to choose tool sets generated by the optimisation. This behaviour is highlighted in Figure 4, which illustrates the iterative behaviour of the mandrel radius r_m and the final radius r_1 over the iterations of the optimisation. Additionally, the respective resulting extrusion strain ε_{ex} is presented as well. Finally, the upper bounds for the respective radii are indicated to highlight that these bounds never explicitly apply to their respective design variables throughout the optimisation. The figure only shows the behaviour up to iteration 42. After that point in the optimisation, no notable changes in design occur, which is also detectable in the small development of the objective function, again see Figure 3. After a few initial iterations, the optimiser starts to increase the extrusion strain by, at first, reducing the respective radii. The depicted initial constant design variables, that is, the constant values of r_m and r_1 for iterations 0 to 2, are a result of the Nelder-Mead Simplex algorithm. As for this implementation, only the current optimal solution of each iterative step is stored. This might be in turn the initial starting guess as other points of the simplex may yield higher objective values. The following change to the extrusion strain of $\varepsilon_{ex} = 1.35$ at iteration 3 is achieved by reducing the mandrel and final radius, respectively. After this initial change, the radii show some positive and negative adjustments up to iteration 12.

RIGHTSLINK

16177061, 2023, 3, Downloaded from https://onlinelibrary.wiley.com/doi/10.1002/pamm.202300199 by Technische Universitaet Dortmund Dezernat Finanzen und Beschaffung, Wiley Online Library on [24/10/2024]. See the Terms and Conditions (https://onlinelibrary.wiley.com/terms-and-conditions) on Wiley Online Library for rules of use; OA articles are governed by the applicable Creative Commons License

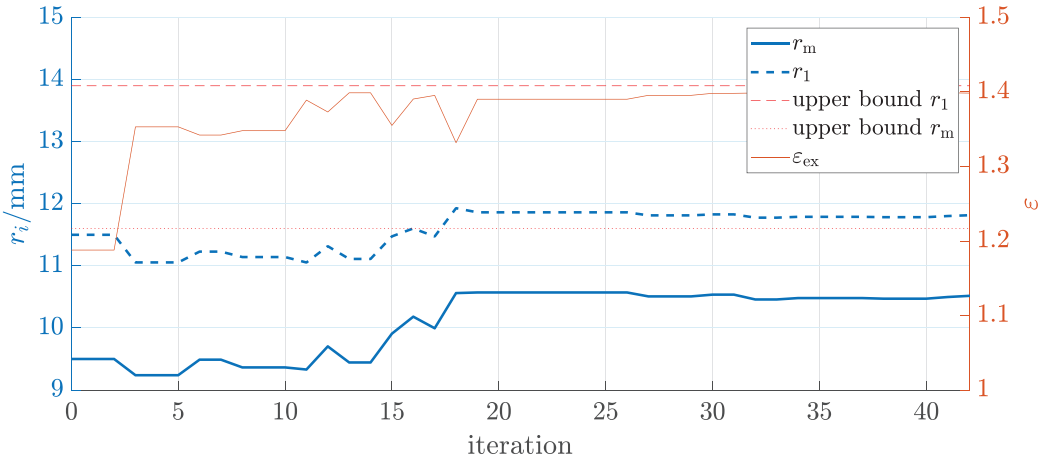

FIGURE 4 An iterative display of the mandrel radius r_m and the final radius r_1 over the iterations up to iteration 42. Additionally, their respective upper bounds and the resulting extrusion strain ε_{ex} for each iteration are depicted.

At this point in the optimisation, the behaviour regarding the radii changes drastically and their respective values start to increase in value by up to 1 mm. The peak of this behaviour is reached at iteration 18. From thereon the optimiser only makes small changes and again decreases their respective values. This coincides with the small changes of the objective function, as was discussed regarding Figure 3. After iteration 26, the radii get reduced again which in turn increases the extrusion strain. This behaviour repeats until iteration 41, after which a final small increase in design is visible. A few intermediate iterations show points, where the extrusion strain decreases. Most notably this occurs at iterations 12, 15 and 18, respectively. At these iterations the iterative optimal solution showed a lower shoulder angle, which in turn benefits the triaxiality value. Subsequently, this angle remains constant for a few iterations while the extrusion strain increases again. A value close to the optimum, that is, $2\alpha = 30.162°$, is finally reached at iteration 18. Afterwards, the extrusion strain exceeds the value of $\varepsilon_{ex} = 1.39$ again and does not fall below that threshold throughout the rest of the optimisation.

Additional calculations were performed to underline this result, that is, the objective having a lower value between the bounds of the radii rather than at either limit. Further optimisations with different starting values at the upper boundaries however deemed difficult because the optimiser often ran into iterative solutions which did not converge for the FE problem due to high mesh distortions. However, at best, the possible manual calculations, as well as intermediate results from the additional optimisations, generates values close to $\eta^{mean} = -1.999$, indicating an overall better solution obtained by the optimisation as described above.

4 | SUMMARY AND OUTLOOK

This contribution presented a generalised optimisation framework surrounding a commercial finite element software. The application of Abaqus FAE was motivated by the necessity to consider contact for accurate modelling of forming processes. The proposed framework, with possible alternative approaches and their drawbacks, were presented. It was applied to hollow forward rod extrusion to yield optimal process parameter sets with the objective, to generate workpieces with a reduced accumulation of ductile damage. Interestingly, a non-intuitive combination of radii was generated, that lay at neither bound of their respective variable, highlighting the benefit of utilising numerical optimisation.

Based on the conducted investigations in this paper, there are many additional directions of research to be considered. For one, the optimal set of process parameters could be directly validated by manufacturing tool sets with the properties generated in the optimisation. Additionally, the optimisation of hollow forward extrusion can be extended by for example, including the omitted process parameters as additional design variables. Due to the generalisation of the proposed optimisation framework, the forming processes to be optimised are not limited to extrusion processes. Natural extensions on this regard are sheet metal forming processes like deep-drawing or roll-forming, or hot forging process which take temperature effects into consideration.

RIGHTSLINK

16177061, 2023, 3, Downloaded from https://onlinelibrary.wiley.com/doi/10.1002/pamm.202300199 by Technische Universitaet Dortmund Dezernat Finanzen und Beschaffung, Wiley Online Library on [24/10/2024]. See the Terms and Conditions (https://onlinelibrary.wiley.com/terms-and-conditions) on Wiley Online Library for rules of use; OA articles are governed by the applicable Creative Commons License

ACKNOWLEDGMENTS

The financial support of the Deutsche Forschungsgemeinschaft (DFG, German Research Foundation) for projects A02 and C05 within the Collaborative Research Centre TRR 188 – Projektnummer 278868966 "Damage Controlled Forming Processes" is gratefully acknowledged.

Open access funding enabled and organized by Projekt DEAL.

ORCID

Fabian Guhr https://orcid.org/0000-0002-3341-0503

REFERENCES

1. Rogers, H. (1960). The tensile fracture of ductile metals. *Transactions of the metallurgical society of AIME*, *218*, 498–506.
2. Tekkaya, A. E., Ben Khalifa, N., Hering, O., Meya, R., Myslicki, S., & Walther, F. (2017). Forming-induced damage and its effects on product properties. *Cirp Annals-manufacturing Technology*, *66*, 281–284.
3. Hering, O., Dunlap, A., Tekkaya, A. E., Aretz, A., & Schwedt, A. (2020). Characterization of damage in forward rod extruded parts. *International Journal of Material Forming*, *13*, 1003–1014.
4. Guhr, F., Sprave, L., Barthold, F.-J., & Menzel, A. (2020). Computational shape optimisation for a gradient-enhanced continuum damage model. *Computational Mechanics*, *65*, 1105–1124.
5. Guhr, F., & Barthold, F.-J. (2023). Geometric and material sensitivities for elasto-plasticity including non-local damage regularisation. *Proceedings in Applied Mathematics and Mechanics*, *23*, e202200233.
6. Noël, L., Duysinx, P., & Maute, K. (2017). Level set topology optimization considering damage. *Structural and Multidisciplinary Optimization*, *56*, 737–753.
7. Dassault Systèmes (2023). Simulia Abaqus manual. https://help.3ds.com/2023/English/DSSIMULIA_Established/SIMULIA_Established_FrontmatterMap/sim-r-DSDocAbaqus.htm?contextscope=all
8. Barthold, F.-J. (2008). Remarks on variational shape sensitivity analysis based on local coordinates. *Engineering Analysis with Boundary Elements*, *32*, 971–985.
9. Liedmann, J., Gerke, S., Barthold, F.-J., & Brünig, M. (2020). Shape optimization of the X0-specimen: theory, numerical simulation and experimental verification. *Computational Mechanics*, *66*, 1275-1291.
10. Liedmann, J., & Barthold, F.-J. (2020). Variational sensitivity analysis of elastoplastic structures applied to optimal shape of specimens. *Structural and Multidisciplinary Optimization*, *61*, 2237–2251.
11. Stavroulakis, G. E. (1995). Optimal prestress of structures with frictional unilateral contact interfaces. *Archive of Applied Mechanics*, *66*, 71–81.
12. Hilding, D., & Klarbring, A. (2012). Optimization of structures in frictional contact. *Computer Methods in Applied Mechanics and Engineering*, *205–208*, 83–90.
13. Guhr, F., & Barthold, F.-J. (2021). Damage optimisation for air bending. *Proceedings in Applied Mathematics and Mechanics*, *20*, e202000074.
14. Guhr, F., & Barthold, F.-J. (2019). Load Optimisation for Damage Reduction and Fracture Prevention. *Proc. 8th GACM*, *8*, 55–58.

How to cite this article: Guhr, F., Gitschel, R., Barthold, F.-J., & Tekkaya, A. E. (2023). Numerical optimisation of damage in extrusion processes. *Proceedings in Applied Mathematics and Mechanics*, *23,* e202300199. https://doi.org/10.1002/pamm.202300199

16177061, 2023, 3, Downloaded from https://onlinelibrary.wiley.com/doi/10.1002/pamm.202300199 by Technische Universitaet Dortmund Dezernat Finanzen und Beschaffung, Wiley Online Library on [24/10/2024]. See the Terms and Conditions (https://onlinelibrary.wiley.com/terms-and-conditions) on Wiley Online Library for rules of use; OA articles are governed by the applicable Creative Commons License

RIGHTSLINK